Available online at www.sciencedirect.com

SciVerse ScienceDirect

Procedia Engineering 57 (2013) 1205 – 1212

Procedia Engineering

www.elsevier.com/locate/procedia

11th International Conference on Modern Building Materials, Structures and Techniques, MBMST 2013

Evaluation of Time Loading Influence on Asphalt Pavement Rutting

Audrius Vaitkus[a,]*, Miglė Paliukaitė[b]

[a,b]Road Research Institute, Vilnius Gediminas Technical University, Linkmenų str. 28, LT-08217 Vilnius, Lithuania

Abstract

The rutting of asphalt pavement structures during their exploitation is considered to be one of the main problems in Lithuania, as well as in the entire world. This kind of pavement distress makes a negative impact to the exploitation characteristics of the asphalt pavement, to the residual life of pavement structure, also to the safety and quality of the traffic. The main purpose of this analysis is to define the resistance to rutting of various kinds of pavement structures and to assess the variation of rut depth in dependence on the traffic loading (number of equivalent standard axel loads – ESAL's). The analysis is performed and is still continued at the road of experimental pavement structures, where 27 different pavement structures were installed. The statistical analysis of the rut depth let to define the most precise criterion for the assessment of every kind of pavement – meridian.

Keywords: asphalt pavement structure; pavement distress; ruts(-ing); ESAL's; pavement residual life.

1. Introduction

Safwan and Tamer [1] analysed the rut formation prognosis model (The Ohio state model). This model is the linear dependence between the stress and repeated loading number logarithm, which parameters depend on the kind of material. The Ohio state model can be used to forecast the rut formation and to compare the behaviour of various asphalt mixes during the rut formation process. Using this model, the analysis and assessment of four different asphalt mixes rutting potential, using asphalt mixtures with narrow and wide aggregate particle distribution, was made. Rashid K. Abu Al-Rub [2] also analysed the prediction of rutting in asphalt pavements under repeated loading conditions comparing finite element and constitutive modelling techniques, i.e. he evaluated the difference between 2D and 3D simulations and the effect of different performance loading assumptions (e.g. pulse loading and equivalent loading) on the predicted rut depth. Results showed that the 2D plane strain FE simulations significantly overestimate rutting as compared with the rutting performance predictions from more realistic 3D FE simulations. 3D FE models have also been used for the evaluation of the effects of various bonding conditions on the overlay response as well as the interface behaviour. This study found that as pavement temperature increases, the interface bonding effects on the overlay response are amplified. This could be the main contributing factor to overlay rutting [3]. Motiejūnas [4] made an assessment of temperature distribution in the different layers of asphalt pavement dependence on environmental temperature as well as the influence of the temperature variation for the stiffness of asphalt layers. Temperature is one of the most dominant factors that impact the variation in modulus of asphalt layers. Nazarian and Alvarado [14] analysed the relationship between temperature and modulus of AC layers. Getautis and Sivilevičius [5] statistical analysis showed that the highest rut depth is formed at the first traffic lane in the pathway zone of the right wheel of the vehicle. As well as in this zone the rutting was the most uneven.

* Corresponding author.
E-mail address: audrius.vaitkus@vgtu.lt

doi:10.1016/j.proeng.2013.04.152

It is known that variations in material characteristics are a major factor to influence the rutting resistance of asphalt mixtures [17]. Many researchers have performed a lot of work on it [15], [18]. At the same time, different test methods were utilized to estimate the rutting performance of asphalt pavement. Visco-elasticity theory, especially linear visco-elasticity models, have been developed to predict the rutting in asphalt pavements [19].

Arabani [6] suggested two ways how to increase the durability of asphalt pavement structure: first is to increase the total thickness of asphalt layers, second is to use the polymer modified bitumen during the construction process of asphalt pavement. Jan Ritter [7], [20] defined, that at the thinner asphalt layers the considerable decrease the strength of pavement structure as well as increases the crack formation in the asphalt base layers. The modification of asphalt mix with polymer or other additives increase the durability of asphalt pavement and decrease the rutting [8-9]. Vaitkus [10] ascertained that the usage of particular supplements in warm mix asphalt increases the stiffness of the binder and at the same time improves the resistance to rutting. The dynamic creep compression tests for bituminous materials with different air void contents under different stress levels were carried out and the study indicated that air void contents have significant influence on the behaviour of rutting under wheel loadings [15].

1.1. Road of experimental pavement structures

In 2007 near Vilnius City in Pagiriai settlement the road of experimental pavement structures was constructed. The parameters of experimental pavement structures road's transverse profile according to STR 2.06.03:2001corresponds to the III category (2 traffic lines, pavement width – 7m, roadside width – 1m) and the III class of pavement structure class (ESAL's of 100 kN = (0,8–3,0) million). The road of experimental pavement structures, which is in total 710 m long, consists of 23 sectors of 30 m long and one 20 m long sector. Three sectors additionally are divided into 15 m sections. The pavement structures of various kinds were constructed at these sectors. The experimental road was constructed on the way to gravel quarry where the empty heavy vehicle are going in and the loaded are going out. In this case, the one traffic lane of the experimental road is loaded much more than the other [11].

Various materials were used for every layer of experimental road sector construction. The frost blanket layer was built from sand (0/4, 0/11); the base layer from 0/32, 0/56 crushed dolomite and granite, the mix of crushed granite and sand, crushed gravel mix, gravel and sand mix) and the reclaimed asphalt. The asphalt base layer was built from 0/32-C (AC11PS) (crushed dolomite and gravel); asphalt binder layer: 0/16-A (AC16AS), 0/16-APMB (AC16AS PMB) (crushed dolomite, crushed granite, crushed gravel and sand); asphalt wearing layer: 0/11 S-V (AC11VS), 0/11 S-M (SMA11S), 0/11 S-M PMB (SMA11S PMB), Confalt [12].

The thickness and materials for every pavement construction were chosen according to reference pavement structure, which was made from asphalt wearing layer 0/11 S-V (AC11VS); asphalt binder layer 0/16-A (AC16AS); asphalt base layer 0/32-C (AC32PS); base layer – crushed dolomite 0/56; frost blanket layer – sand 0/11, see Fig. 1. The all combinations of the materials of different sectors are presented in Table 1 [13].

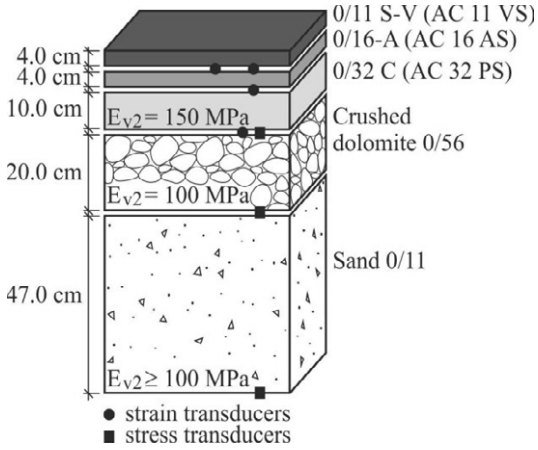

Fig. 1. Reference pavement structure (No 19)

The traffic flow is registering consistently after the first car passed after opening of the road. For the classification of traffic flow the induction loops, installed into road pavement, were used as well as the Loop profiler classificator. All vehicle were normed under ESAL's$_{100}$=100 kN. ESAL's$_{100}$ distribution at the time of experimental sector's use is presented

in Fig. 2. The experimental road is used by 70000 ESAL's$_{100}$ in average annually, total amount of ESAL's100 since the beginning of road exploitation until the end of 2011 is 300000.

Table 1. The materials used for pavement structure construction

No of pavement structure	Asphalt wearing layer (thickness, cm)	Asphalt binder layer (thickness, cm)	Asphalt base layer (thickness, cm)	Base layer (thickness, cm)		Frost blanket layer (thickness, cm)
1	0/11 S-V AC 11VS (4 cm)	0/16 A AC 16 AS (4 cm)	0/32 C AC 32 PS (14 cm)	0/32 Gravel-sand mix (20 cm)		0/11 Sand (43 cm)
2	0/11 S-V AC 11VS (4 cm)	0/16 A AC 16 AS (4 cm)	0/32 C AC 32 PS (10 cm)	0/56 Crushed dolomite (15 cm)	0/32 Gravel-sand mix (20 cm)	0/11 Sand (32 cm)
3	0/11 S-V AC 11VS (4 cm)	0/16 A AC 16 AS (4 cm)	0/32 C AC 32 PS (10 cm)	0/56 Crushed dolomite (30 cm)		0/4 Sand (37 cm)
4	0/11 S-V AC 11VS (4 cm)	0/16 A AC 16 AS (4 cm)	0/32 C AC 32 PS (10 cm)	0/56 Crushed dolomite (20 cm)		0/4 Sand (47 cm)
5	0/11 S-V AC 11VS (4 cm)	0/16 A AC 16 AS (4 cm)	0/32 C AC 32 PS (10 cm)	Aggregate – milled asphalt concrete (10 cm)	0/32 Crushed dolomite (10 cm)	0/11 Sand (47 cm)
6	0/11 S-V AC 11VS (4 cm)	0/16 A AC 16 AS (4 cm)	0/32 C AC 32 PS (10 cm)	0/32 Gravel-sand mix (20 cm)		0/11 Sand (47 cm)
7	0/11 S-V AC 11VS (4 cm)	0/16 A AC 16 AS (4 cm)	0/32 C AC 32 PS (10 cm)	0/32 Crushed granite and sand mix (20 cm)[8]		0/11 Sand (47 cm)
8	0/11 S-V AC 11VS (4 cm)	0/16 A AC 16 AS (4 cm)	0/32 C AC 32 PS (10 cm)	0/56 Crushed granite (20 cm)		0/11 Sand (47 cm)
9	Confalt (4 cm)	0/16 A AC 16 AS (4 cm)	0/32 C AC 32 PS (10 cm)	0/56 Crushed dolomite (20 cm)		0/11 Sand (47 cm)
10	0/11 S-M SMA 11 S (4 cm)	0/16 A AC 16 AS (4 cm)	0/32 C AC 32 PS (10 cm)	0/56 Crushed dolomite (20 cm)		0/11 Sand (47 cm)
11	0/11 S-M$_{(PMB}$[11]$_{)}$ SMA 11 S (4 cm)	0/16 A$_{PMB}$ AC 16 AS (4 cm)	0/32 C AC 32 PS (10 cm)	0/56 Crushed dolomite (20 cm)		0/11 Sand (47 cm)
12	0/11 S-M $_{(PMB)}$ SMA 11 S (4 cm)	0/16 A AC 16 AS (4 cm)	0/32 C AC 32 PS (10 cm)	0/56 Crushed dolomite (20 cm)		0/11 Sand (47 cm)
13	0/11 S-V AC 11VS (4 cm)	0/16 A[1] AC 16 AS (4 cm)	0/32 C AC 32 PS (10 cm)	0/56 Crushed dolomite (20 cm)		0/11 Sand (47 cm)
14	0/11 S-V AC 11VS (4 cm)	0/16 A[2] AC 16 AS (4 cm)	0/32 C AC 32 PS (10 cm)	0/56 Crushed dolomite (20 cm)		0/11 Sand (47 cm)
15	0/11 S-V AC 11VS (4 cm)	0/16 A[3] AC 16 AS (4 cm)	0/32 C AC 32 PS (10 cm)	0/56 Crushed dolomite (20 cm)		0/11 Sand (47 cm)
16	0/11 S-V AC 11VS (4 cm)	0/16 A[4] AC 16 AS (4 cm)	0/32 C AC 32 PS (10 cm)	0/56 Crushed dolomite (20 cm)		0/11 Sand (47 cm)
17	0/11 S-V AC 11VS (4 cm)	0/16 A[5] AC 16 AS (4 cm)	0/32 C AC 32 PS (10 cm)	0/56 Crushed dolomite (20 cm)		0/11 Sand (47 cm)
18	0/11 S-V AC 11VS (4 cm)	0/16 A[6] AC 16 AS (4 cm)	0/32 C AC 32 PS (10 cm)	0/56 Crushed dolomite (20 cm)		0/11 Sand (47 cm)
19	0/11 S-V AC 11VS (4 cm)	0/16 A AC 16 AS (4 cm)	0/32 C AC 32 PS (10 cm)	0/56 Crushed dolomite (20 cm)		0/11 Sand (47 cm)
20	0/11 S-V AC 11VS (4 cm)	0/16 A[9] AC 16 AS (4 cm)	0/32 C[9] AC 32 PS (10 cm)	0/56 Crushed dolomite (20 cm)		0/11 Sand (47 cm)
21	0/11 S-V AC 11VS (4 cm)	0/16 A[9] AC 16 AS (4 cm)	0/32 C[9] AC 32 PS (10 cm)	0/56 Crushed dolomite (20 cm)		0/11 Sand (47 cm)
22	0/11 S-V AC 11VS (4 cm)	0/16 A[9] AC 16 AS (4 cm)	0/32 C[9] AC 32 PS (10 cm)	0/56 Crushed dolomite (20 cm)		0/11 Sand (47 cm)
23	0/11 S-V AC 11VS (4 cm)	0/16 A AC 16 AS (4 cm)	0/32 C AC 32 PS (10 cm)	0/56 Crushed dolomite (20 cm)		0/11 Sand (47 cm)
24	0/11 S-V AC 11VS (4 cm)	0/16 A AC 16 AS (4 cm)	0/32 C AC 32 PS (10 cm)	0/56 Crushed dolomite (20 cm)		0/11 Sand (47 cm)[10]
25	0/11 S-V AC 11VS (4 cm)	0/16 A AC 16 AS (4 cm)	0/32 C AC 32 PS (10 cm)	0/56 Crushed dolomite (20 cm)		0/11 Sand (47 cm)
26	0/11 S-V AC 11VS (4 cm)	0/16 A AC 16 AS (4 cm)	0/32 C[6] AC 32 PS (10 cm)	0/56 Crushed dolomite (20 cm)		0/11 Sand (47 cm)
27	0/11 S-V AC 11VS (4 cm)	0/16 A AC 16 AS (4 cm)	0/32 C[7] AC 32 PS (10 cm)	0/56 Crushed dolomite (20 cm)		0/11 Sand (47 cm)

1. crushed granite 11/16 + crushed dolomite 5/8 + (crushed dolomite and crushed granite 8/11, 50% and 50%);
2. crushed granite 8/11 and 11/16 + crushed gravel (rest of aggregates);
3. crushed dolomite 8/11 and 11/16 + crushed gravel (rest of aggregates);
4. 50 % crushed granite + 50 % sand
5. 100 % crushed granite
6. 100 % crushed gravel
7. 50 % crushed dolomite + 50 % crushed gravel

8. 50 % crushed granite + 50 % sand and gravel mix
9. geosynthetics between asphalt binder layer and asphalt base layer
10. geosynthetics between base layer and frost blanket layer
11. PMB (polymer modified bitumen)

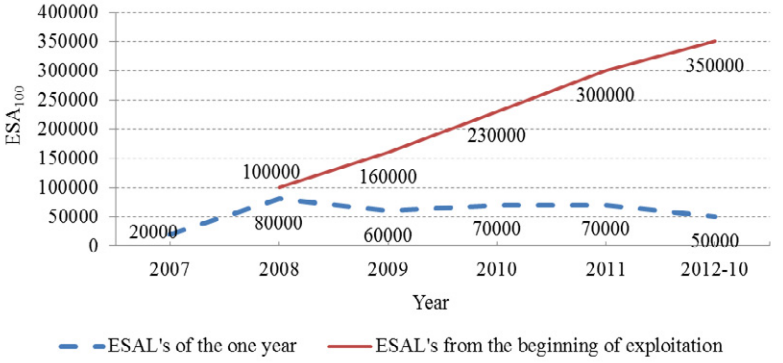

Fig. 2. Distribution of ESAL‘s_{100} of road experimental pavement structures

Every year at the experimental road sector these measurements are made:

- measurement of traffic flow;
- measurement of temperature and moisture in different layers of pavement structure;
- measurement of rutting;
- visual assessment of pavement distress;
- measurement of pavement roughness;
- measurement of pavement skid resistance;
- measurement of pavement equivalent modulus with Falling Weight Deflectometer;
- measurement of pavement deflection with Benkelman Beam.

This article analysis the results of asphalt pavement structure rutting then the experimental sector was used by ESAL‘s_{100}=180000, ESAL‘s_{100}=230000, ESAL‘s_{100}=250000, ESAL‘s_{100}=290000.

2. The experimental research and analysis of the results

The rut depth of asphalt pavement structure of experimental road is measuring in both traffic lanes – loaded and unloaded. The measurements are made by mobile road research laboratory RST-28. The rut depth is measured using laser sensors that measure the transverse road profile at particular intervals and ensure the sufficient reliability for the definition of rut depth.

The measurements of rut depth are made every 1 m, 30 values in total. The average depth of the right, the left rut and the maximum clearance was counted at every sector. To increase the precision of the measurements and to get the reliable analysis results the additional statistical analysis was made. This analysis let to define the most relevant statistical index which shows the proper meaning of the rut depth in every measured sector. For the definition of rut depth proper meaning the statistical analysis of these grip description criterion was made: median, mode, the average of 20 section measurement data, the average of 30 section measurement data.

The one kind of statistical analysis covered the assessment of 20 meters average measurements of every section. In this case in every 30 m long section was assessed only these values which were received rejecting the first 5 and the last 5 meters of measurement data. So the possible errors, which could occur because of the connection of different pavement structures, were eliminated. The distribution of rut depth in different pavement structures dependent on statistical criterion when the experimental road was passed by ESAL‘s_{100}=180000, ESAL‘s_{100}=230000, ESAL‘s_{100}=250000, ESAL‘s_{100}=290000 are presented in Fig. 3-6.

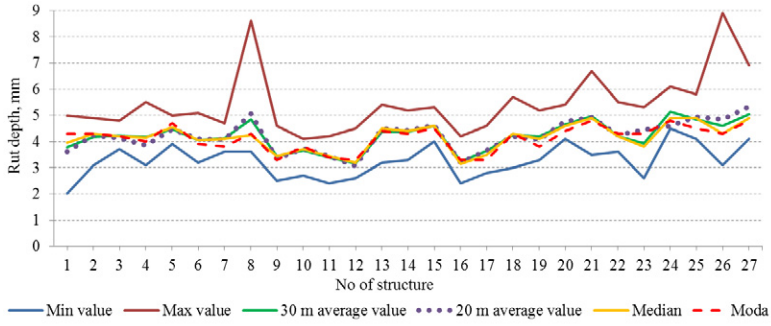

Fig. 3. Distribution of rut depth in different pavement structures dependent on statistical criterion ESAL‘s_{100}=180000

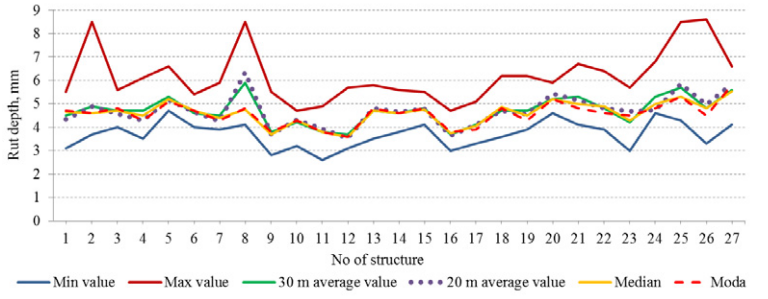

Fig. 4. Distribution of rut depth in different pavement structures dependent on statistical criterion ESAL‘s_{100}=230000

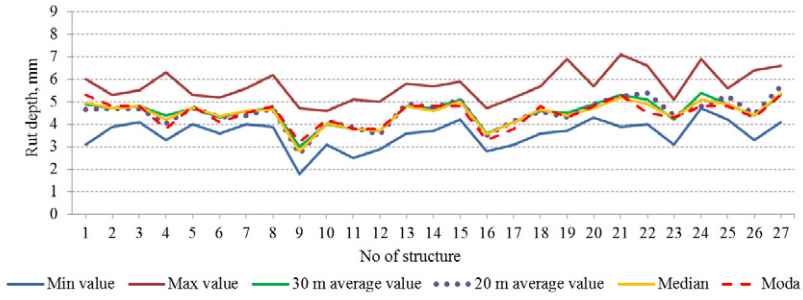

Fig. 5. Distribution of rut depth in different pavement structures dependent on statistical criterion ESAL‘s_{100}=250000

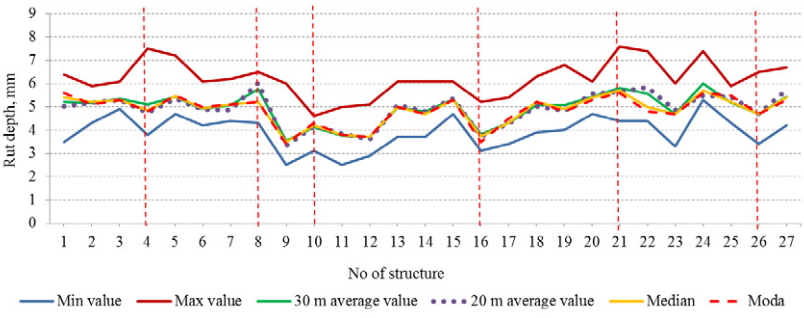

Fig. 6. Distribution of rut depth in different pavement structures dependent on statistical criterion ESAL‘s_{100}=290000

The assessment of the loaded traffic lane right rut depth measurement, i.e. comparing the differences between the minimal and maximal values, the average of rut depth in 30 m and 20 m sections, the median and mode the extreme points

were defined. The extreme points most visible at ESAL's_{100}=290000, see Fig. 6. These pavement structures were defined: 4th, 8th, 9th, 16th, 21th and 26th (Table 1.). The analysis of rut depth dependence on ESAL's let to define that rut depth increases proportionally ESAL's. The highest rut depth were measured at ESAL's_{100}=290000; the lowest at ESAL's_{100}=180000. For the further analysis the results of the 2011 year autumn measurements of rut depth were chosen at ESAL's_{100}=290000. All the 27 pavement structures were analysed and the most proper rut depth measurement statistical criterion was defined. The Fig. 7 presents the comparison of rut depth statistical criterion assessment of pavement structure (sector no. 19).

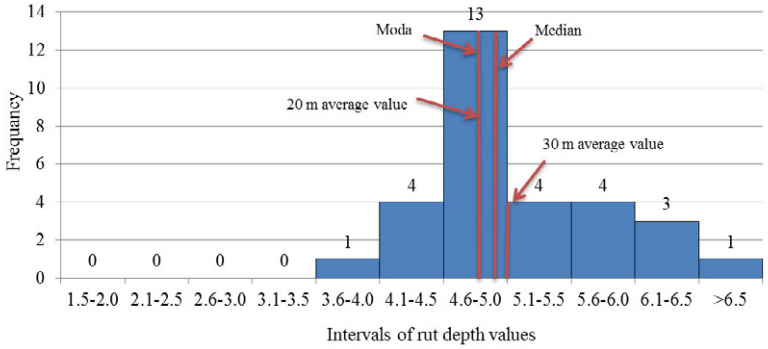

Fig. 7. The comparison of rut depth assessment statistical criterion of the pavement structure of the 19th sector

The statistical analysis of the rut depth let to define that median has a 0.30 mm (0.08 mm in average) distinction from mode, the difference from median and average value at 30 m is up to 0.58 mm (0.11 mm in average), the difference between 30 m and 20 m average values is up to 0.51 mm (0.15 mm in average), the difference between the minimal and maximal values – up to 11.30 mm (average 2.66 mm). Also it was defined:

- There is a great difference between minimal and maximal values of rut depth;
- There is almost no difference of the average value at 30 m and 20 m (then 5 m from the beginning and the end of the section were eliminated), it means that connection of different pavement structure has no influence to rut depth;
- The median and the average value of rut depth at 30 m has a great difference (up to 0.58 mm), this is because there is a great difference between the minimal and the maximal rut depth values that misrepresent the total value of 30 m rut depth.
- The median and the mode have a little difference (up to 0.30 mm), but evaluating all rut depth values the median is more precise than mode. For the further analysis the median criterion of every section was accepted.

The distribution of rut depth in different pavement structures dependence on the median criterion is presented in Fig. 8.

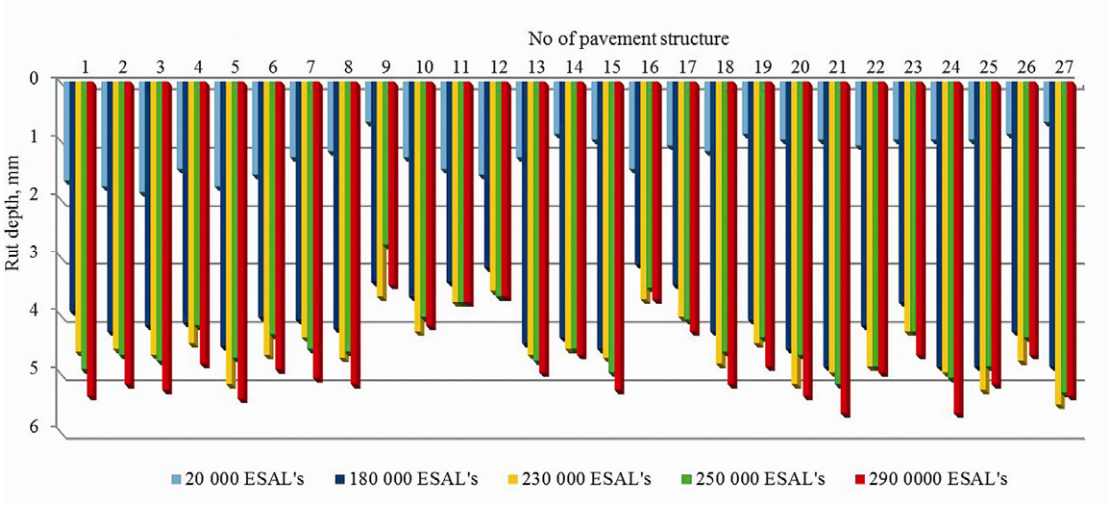

Fig. 8. Distribution of rut depth in different pavement structures dependence on median criterion

Analysis of the measurements of loaded traffic line right rut depth (Fig. 8.) at ESAL's_{100}=180000, ESAL's_{100}=230000, ESAL's_{100}=250000, ESAL's_{100}=290000 and assessment of rut depth according to median defined that the highest depth is at ESAL's_{100}=290000, and the lowest at ESAL's_{100}=200000. The highest rut depth at ESAL's_{100}=290000 were defined: in the 1th (5,4 mm), 5th (5,5 mm), 21th (5,7 mm), 24th (5,7 mm) and 27th (5,4 mm) pavement structures; the lowest: in the 9th (3,5 mm), 10th (4,2 mm), 11th (3,8 mm), 12th (3,7 mm) and 16th (3,8 mm) pavement structure. The comparison of rut depth at ESAL's_{100}=180000, ESAL's100=230000, ESAL's_{100}=250000 and ESAL's_{100}=290000 showed that the pavement structures with the highest and the lowest rut depth remains the same, and only then ESAL's_{100} is rising the rut depth was rising too from 1 mm up to 8 mm.

So it can be affirmed that the rut is formed at the asphalt wearing course. Minimum rut depth was formed in these pavement structures that had asphalt pavement wearing course constructed from Confalt, stone mastic asphalt SMA11S and stone mastic asphalt SMA11S with PMB. The maximum rut depth is formed at these pavement structures which had an asphalt wearing course constructed from AC11VS and asphalt binder layer AC16AS with bitumen 50/70.

3. Conclusions

The asphalt pavement distresses impact the traffic loading, climate and environmental conditions. The most often and negative type of pavement distress is rutting. It significantly depends on type of pavement structure, kind and quality of materials used for different types of structure layers, also pavement construction techniques and quality.

The assessment of loaded traffic line right rut depth measurements i.e. comparing the differences between the minimal and maximal values, the average of rut depth in 30 m and 20 m sections, the average of rut depth at 30 m, median and mode at different number of ESAL's_{100}, let to define that the most accurate way for the rut depth assessment is the median calculation.

The usage of rut depth assessment methodology, i.e. the median calculation at ESAL's_{100}=290000 let to define the highest rut depth at the 1th (5,4 mm), 5th (5,5 mm), 21th (5,7 mm), 24th (5,7 mm) and 27th (5,4 mm) pavement structures; the lowest rut depth at 9th (3,5 mm), 10th (4,2 mm), 11th (3,8 mm), 12th (3,7 mm) and 16th (3,8 mm) pavement structures.

So it could be affirmed that the rut is formed in asphalt wearing course. The minimum rut depth was formed in pavement structures were asphalt wearing course was built from Confalt, stone mastic asphalt SMA11S, stone mastic asphalt SMA11S with PMB. The maximum rut depth was formed in pavement structures were the asphalt wearing course was built from AC11VS and asphalt binder layer AC16AS with bitumen 50/70.

References:

[1] Safwan, A. K.,Tamer, M. B., 2011. Rutting parameters for asphalt concrete for different aggregate structures, International Journal of Pavement Engineering 12(1), pp. 13-23.

[2] Abu Al-Rub, R. K., Darabi, M. K., Huang, C. W., Masad, E. A., Little, D. N., 2012. Comparing finite element and constitutive modelling techniques for predicting rutting of asphalt pavements, International Journal of Pavement Engineering 13(4), pp. 322-338.

[3] Ozer, H., Al-Qadi, I. L., Wang, H., Leng, Z. 2011. Characterisation of interface bonding between hot-mix asphalt overlay and concrete pavements: modelling and in-situ response to accelerated loading, International Journal of Pavement Engineering 13(2), pp. 181-196.

[4] Motiejūnas, A., Palukaitė, M., Vaitkus, A., Čygas, D., Laurinavičius, A., 2010. Research of the Dependence of Asphalt Pavement Stiffness Upon the Temperature of Pavement Layers, The Baltic Journal of Road and Bridge Engineering 5(1), pp. 50-54.

[5] Getautis, E., Sivilevičius, H., 2009. Lietuvos valstybinės reikšmės kelių asfalto dangos provėžų gylio statistinis tyrimas ir vertinimas, Mokslas Lietuvos ateitis = Science-Future of Lithuania, Transport Engineering 1(6).

[6] Arabani, M., Mirabdolazimi, S. M., Sasani, A. R., 2010.The Effect of Waste Tire Thread mesh on the dynamic behaviour of asphalt mixtures, Construction and Building Materials 24(6), pp. 1060-1068.

[7] Ritter, J., Rabe, R., Wolf, A., 2012. Analysis of the long-term structural performance of flexible pavements using full-scale accelerated pavement tests, Transport Research Arena-Europe 2012.

[8] Moghaddam, T. B., Karim, M. R., Abdelaziz, M. 2011. A review on fatigue and rutting performance of asphalt mixes, Scientific Research and Essays 6(4), pp. 670-682.

[9] Kamaruddin, I., Madzlan, B. N., Yasreen, G. S., 2010. The Effect of Fine Aggregate Properties on the Rutting Behavior of the Conventional and Polymer Modified Bituminous Mixtures Using Two Types of Sand as Fine Aggregate. Proceeding of Malaysian Universities Transportation Research Forum and Conferences 2010 (MUTRFC2010), 21 December, 2010, Universiti Tenaga Nasional.

[10] Vaitkus, A., Čygas, D., Laurinavičius, A., Vorobjovas, V., Perveneckas, Z. 2009. Analysis and evaluation of compaction properties of Warm Mix Asphalt, the II International Conference, Environmentally Friendly Roads – Enviroad 2009, Warsow, Poland.

[11] Čygas, D., Laurinavicius, A., Vaitkus, A., Perveneckas, Z., Motiejūnas, A., 2008. Research of Asphalt Pavement Structures on Lithuanian Roads, The Baltic Journal of Road and Bridge Engineering 3(2), pp. 77-83.

[12] Vaitkus, A., Puodžiukas, V., Motiejūnas, A., Vitkienė, J., Vorobjovas, V., Paliukaitė, M., 2010. Long Term Research of Experimental Asphalt Pavement Structures, Transport Research Arena Europe 2010, Brussels, Belgium.

[13] Laurinavičius, A., Vaitkus, A., Bertulienė, L., Tuminienė, F., Žiliūtė, L., 2009. Research of Experimental Road Pavement Structures in Lithuania, the II International Conference Environmentally Friendly Roads - Enviroad 2009, Warsow, Poland.

[14] Nazarian, S., Alvarado, G. 2006. Impact of temperature gradient on modulus of asphaltic concrete layers, Journal of Materials in Civil Engineering 18(4), pp. 492-498.
[15] Suo, Z., Wong, W.G., 2009. Nonlinear properties analysis on rutting behaviour of bituminous materials with different air void contents, Construction and Building Materials 23(12), pp. 3492-3498.
[17] Huang, X. M., Zhang, Y. Q. 2010. A new creep test method for asphalt mixtures, Road Mater Pavement 11(4), pp. 969-991.
[18] Liseane, P.T.L. Fontes, Glicério Trichês, Jorge C. Pais, Paulo A.A. Pereira. 2010. Evaluating permanent deformation in asphalt rubber mixtures, Constraction and Building Materials.24, pp. 1193-1200.
[19] Archilla, A. R. 2006. Use of Superpave Gyratory Compaction Data for Rutting Prediction, Journal of Transportation Engineering 132(9), pp. 734-741.
[20] Tao, X., Xiaoming, H. 2012. Investigation into causes of in-place rutting in asphalt pavement, Construction and Building Materials 28 (2012), pp. 525-530.